




PNPLA3 I148M Variant Impairs Liver X Receptor Signaling and Cholesterol Homeostasis in Human Hepatic Stellate Cells

Francesca Virginia Bruschi ¹, Thierry Claudel,¹ Matteo Tardelli,¹ Patrick Starlinger ², Fabio Marra ³, and Michael Trauner¹

The patatin-like phospholipase domain-containing protein 3 (*PNPLA3*) I148M variant predisposes to hepatic steatosis and progression to advanced liver injury with development of fibrosis, cirrhosis, and cancer. Hepatic stellate cells (HSCs) drive the wound healing response to chronic injury, and lack of liver X receptor (LXR) signaling exacerbates liver fibrogenesis by impairing HSC cholesterol homeostasis. However, the contribution of the I148M variant to this process is still unknown. We analyzed LXR expression and transcriptional activity in primary human HSCs and overexpressing LX-2 cells according to *PNPLA3* genotype (wild type [WT] versus I148M). Here we demonstrate that LXR α protein increased whereas LXR target gene expression decreased during *in vitro* activation of primary human HSCs. Notably, LXR α levels and signaling were reduced in primary I148M HSCs compared to WT, as displayed by decreased expression of LXR target genes. Moreover, reduced expression of cholesterol efflux and enzymes generating oxysterols was associated with higher total and free cholesterol accumulation whereas endogenous cholesterol synthesis and uptake were diminished in I148M HSCs. Luciferase assays on LXR response element confirmed decreased LXR transcriptional activity in I148M HSCs; in contrast the synthetic LXR agonist T0901317 replenished LXR functionality, supported by adenosine triphosphate-binding cassette subfamily A member 1 (*ABCA1*) induction, and reduced collagen1 α 1 and chemokine (C-C motif) ligand 5 expression. Conversely, the peroxisome proliferator-activated receptor gamma (*PPAR γ*) agonist rosiglitazone had only partial effects on the LXR target gene *ABCA1*, and neither diminished expression of proinflammatory cytokines nor increased *de novo* lipogenic genes in I148M HSCs. **Conclusion:** As a consequence of reduced *PPAR γ* activity, HSCs carrying I148M *PNPLA3* show impaired LXR signaling, leading to cholesterol accumulation. The use of a specific LXR agonist shows beneficial effects for diminishing sustained HSC activation and development of liver fibrogenesis. (*Hepatology Communications* 2019;3:1191-1204).

Genetic factors are important for predisposition to and progression of metabolic liver diseases, such as nonalcoholic fatty liver disease (NAFLD).⁽¹⁻³⁾ A single-base polymorphism of the

human patatin-like phospholipase domain-containing protein 3 (*PNPLA3*) gene (I148M/rs738409 C>G) encoding for adiponutrin is an independent risk factor for hepatic steatosis and susceptibility to liver disease

Abbreviations: α -SMA, α -smooth muscle actin; *ABCA1/G1*, adenosine triphosphate-binding cassette subfamily A/G, member 1; *ACAT1*, acyl-coenzyme A:cholesterol acyltransferase 1; *AP-1*, activator protein 1; *CCL*, chemokine (C-C motif), ligand; *CE*, cholesterol ester; *CH25H*, cholesterol 25-hydroxylase; *CYP27A1*, cytochrome P450 family 27, subfamily A, member 1 (sterol 27-hydroxylase); *FASN*, fatty acid synthase; *FBS*, fetal bovine serum; *FC*, free cholesterol; *HMGCR*, 3-hydroxy-3-methylglutaryl coenzyme A reductase; *HSC*, hepatic stellate cell; *IL-8*, interleukin-8; *KO*, knockout; *LDLR*, low-density lipoprotein receptor; *LXR*, liver X receptor; *LXRE*, liver X receptor response element; *mRNA*, messenger RNA; *NAFLD*, nonalcoholic fatty liver disease; *NASH*, nonalcoholic steatohepatitis; *NPC1*, Niemann-Pick disease, type C intracellular cholesterol transporter 1; *PNPLA3*, patatin-like phospholipase domain-containing protein 3; *PPAR γ* , peroxisome proliferator-activated receptor gamma; *PPRE*, peroxisome proliferator response element; *ROSI*, rosiglitazone; *RT-PCR*, real-time polymerase chain reaction; *SCD1*, stearoyl-coenzyme A desaturase 1; *SREBP*, sterol regulatory element-binding protein; *T09*, T0901317; *TC*, total cholesterol; *TGF*, transforming growth factor; *WT*, wild type.

Received December 19, 2018; accepted June 14, 2019.

Additional Supporting Information may be found at onlinelibrary.wiley.com/doi/10.1002/hep4.1395/supinfo.

Supported by the Austrian Science Foundation (grants F3008-B19 and F7310-B21 to M.T.).

progression, such as nonalcoholic steatohepatitis (NASH), alcoholic steatohepatitis, chronic hepatitis C, and hepatocellular carcinoma.^(4,5) Hepatocellular injury, inflammation with recruitment of immune cells, and activation of hepatic stellate cells (HSCs) are key steps in the progression of NASH.⁽⁶⁻⁸⁾ HSC activation includes a metabolic and phenotypic switch from quiescent fat-storing cells toward highly proliferative and reactive myofibroblast-like HSCs, the key drivers of the fibrotic wound healing response.⁽⁹⁾ We have recently uncovered a fundamental role of *PNPLA3* in HSCs to achieve a fully activated phenotype and the impact of the I148M genetic variant to promote inflammatory cytokine release, with subsequent immune cell recruitment, proliferation, and expression of profibrogenic genes in human HSCs.⁽¹⁰⁾

Impaired cholesterol homeostasis leads to free cholesterol (FC) accumulation in HSCs, thus predisposing to toll-like receptor 4 (TLR4) signaling, down-regulation of bone morphogenetic protein and activin membrane-bound inhibitor (BAMBI), and transforming growth factor (TGF)- β -mediated fibrogenesis.⁽¹¹⁻¹³⁾ Two members of the nuclear receptor superfamily, the liver X receptors (LXRs) α and β nuclear receptor subfamily 1, group H, member 3 (NR1H3)/LXR α ⁽¹⁴⁾ and NR1H2/LXR β ,⁽¹⁵⁾ have a pivotal role in control of cholesterol homeostasis and lipid metabolism throughout the human

body.⁽¹⁶⁾ The transcriptional activity of these nuclear receptors is regulated by metabolites of cholesterol, known as oxysterols, and by retinoid X receptor availability to form heterodimer complexes.⁽¹⁷⁾ Remarkably, the two LXR isotypes display distinct function and tissue distribution throughout the body; β is ubiquitously expressed, whereas α is restricted to metabolic organs.^(18,19) In the liver, transcripts of LXR α and LXR β were found in both parenchymal and nonparenchymal cells.⁽²⁰⁻²²⁾ LXRs have received considerable attention as possible candidates for therapeutic approaches in metabolic diseases due to LXR α -mediated induction of bile acid synthesis, hepatic *de novo* lipogenesis, and reduction of high-density lipoprotein cholesterol in LXR α knockout (KO) mice.⁽²³⁻²⁷⁾ In particular, lack of LXR exacerbated liver fibrosis in two different mouse models of chronic liver injury. HSCs isolated from LXR KO mice showed altered lipid partitioning, as reported, by enlarged lipid droplet accumulation compared to wild-type (WT) cells and enhanced expression of inflammatory and fibrotic molecules, such as collagen1 α 1, monocyte chemoattractant protein 1, and platelet-derived growth factor β .⁽²¹⁾ Of note, *PNPLA3* expression is controlled by LXR/sterol regulatory element-binding protein 1c (SREBP-1c), thus suggesting the tight regulation of this protein along with *de novo* lipogenesis,

© 2019 The Authors. *Hepatology Communications* published by Wiley Periodicals, Inc., on behalf of the American Association for the Study of Liver Diseases. This is an open access article under the terms of the Creative Commons Attribution License, which permits use, distribution and reproduction in any medium, provided the original work is properly cited.

View this article online at wileyonlinelibrary.com.

DOI 10.1002/hep4.1395

Potential conflict of interest: Dr. Trauner consults for, is on the speakers' bureau for, and received grants from Falk, Gilead, Intercept, and MSD; he consults for and received a grant from Albireo, and consults for Genfit, Phenex, Novartis, Bristol-Myers Squibb, and Regulus; he is on the speakers' bureau for and received travel grants from Roche, received grants from Cymabay Takeda, and is coinventor of patents on the medical use of norUDCA. The other authors have nothing to report.

ARTICLE INFORMATION:

From the ¹Hans Popper Laboratory of Molecular Hepatology, Division of Gastroenterology and Hepatology, Department of Internal Medicine III, Medical University of Vienna, Vienna, Austria; ²Department of Surgery, Medical University of Vienna, Vienna, Austria; ³Clinical Pathophysiology Department, University of Florence, Florence, Italy.

ADDRESS CORRESPONDENCE AND REPRINT REQUESTS TO:

Michael Trauner, M.D.
Division of Gastroenterology and Hepatology
Department of Internal Medicine III
Medical University of Vienna

Wahringer Guertel 18-20
A-1090 Vienna, Austria
E-mail: michael.trauner@meduniwien.ac.at
Tel.: +43 1 40 40047410

at least in hepatocytes.⁽²⁸⁾ Moreover, peroxisome proliferator-activated receptor gamma (PPAR γ) positively controls LXR α , thus favoring cholesterol efflux from foam cells.⁽²⁹⁾ HSCs expressing the variant of *PNPLA3* (I148M) showed that decreased PPAR γ signaling up-regulates proinflammatory molecule production and release through enhanced transcriptional activity of activator protein 1 (AP-1) by means of c-Jun N-terminal kinase.⁽¹⁰⁾ These observations encouraged us to explore the hypothesis that I148M *PNPLA3* might impair the crosstalk between PPAR γ and LXR, a master regulator of *de novo* lipogenesis and cholesterol homeostasis in the liver.^(26,27)

Therefore, our aim was to evaluate whether the genetic variant of *PNPLA3* contributes to altered LXR signaling in human HSCs in order to further uncover potential novel therapeutic strategies targeting the molecular and metabolic changes in patients with *PNPLA3* I148M.

Materials and Methods

HUMAN HSC ISOLATION AND CELL CULTURE

HSCs were isolated from donor livers unsuitable for transplantation or liver resections for metastasis of colorectal cancer, as approved by the ethics committees of the University of Florence⁽¹⁰⁾ and the Medical University of Vienna (Ethic Committee number 2032/2013). HSCs were seeded on uncoated plastic dishes and cultivated with Iscove's modified Dulbecco's medium (EuroClone, Italy) supplemented with 20% fetal bovine serum (FBS), 1% glutamine 200 mM, sodium pyruvate 100 mM, nonessential amino acid solution 100X, and antibiotic antimycotic solution 100X (Gibco Life Technologies, Carlsbad, CA). Primary HSCs between passages one and eight were used for this study. For comparison, primary WT and I148M *PNPLA3* HSCs were used at the same passage. The genotype of each isolated HSC line has been analyzed by real-time polymerase chain reaction (RT-PCR) for the I148M single-nucleotide polymorphism, as done routinely in our clinical research center. Only homozygote genotypes (n = 3) were used in this study (C/C as WT and G/G as I148M).

Stably overexpressing WT and I148M LX-2 were generated in our laboratory, as described,⁽¹⁰⁾ and cultured with Dulbecco's modified Eagle's medium (Gibco) supplemented with 5% FBS and 1% penicillin/streptomycin solution (EuroClone).

For cell culture treatments, cells deprived of FBS for 24 hours were stimulated with 10 μ M of specific LXR agonist (T0901317 [T09]; Sigma-Aldrich), inverse agonist (SR9238; Tocris), antagonist (GSK2033; Tocris), and PPAR γ agonist (rosiglitazone [ROSI]; Sigma-Aldrich) for an additional 24 hours.

WESTERN BLOT ANALYSIS

Whole-cell extracts were obtained using radio immunoprecipitation assay buffer (150 mM NaCl, 1% Triton X-100, 0.5% sodium deoxycholate, 0.1% sodium dodecyl sulfate, and 50 mM Tris, pH 8.0) containing complete ethylene diamine tetraacetic acid-free protease inhibitor cocktail tablets (Roche Diagnostics GmbH, Germany) and phosphatase inhibitors (20 mM b-glycerophosphate, 10 mM 4-nitrophenylphosphate, and 50 mM sodium vanadate; Sigma-Aldrich). Primary antibodies as follows were diluted in 3% bovine serum albumin tris-hydroxymethylaminomethane-buffered saline Tween 1X solution at different concentrations: rabbit polyclonal to SREBP-2, 3-hydroxy-3-methylglutaryl coenzyme A reductase (HMGCR), and LXR α (Novus NB300-612) (1:500; all from Santa Cruz Biotechnology); mouse monoclonal to LXR β (1:500; Santa Cruz Biotechnology); rabbit monoclonal to low-density lipoprotein receptor (LDLR) (1:1,000; Abcam, Cambridge, United Kingdom); and rabbit polyclonal to calnexin and β -actin (1:10,000; Sigma-Aldrich). Proteins were detected by enhanced chemiluminescence (GE Amersham, Arlington Heights, IL).

CHOLESTEROL MEASUREMENTS

For lipid extraction and analysis, approximately 1×10^6 cells carrying the two distinct *PNPLA3* genotypes were harvested and resuspended in 200 μ L solution containing chloroform:isopropanol:nonyl phenoxypolyethoxyethanol (NP-40) (7:11:0.1) in a microhomogenizer. Thereafter, the extract was centrifuged for 10 minutes at 15,000g and the liquid

phase was isolated and dried at 50°C for 30 minutes to remove traces of organic solvent. Once dried, the lipids were dissolved in the specific assay buffer, and total cholesterol (TC) and FC were quantified using a colorimetric assay kit (ab65359; Abcam) according to the manufacturer's instructions.

LUCIFERASE ASSAY

Stably overexpressing WT or I148M LX-2 were seeded in a 24-well plate and transiently transfected with 0.3 µg/well of an AP-1, LXR response element (LXRE)-luciferase or peroxisome proliferator response element (PPRE)-luciferase construct using Fugene transfection reagent (Promega, Madison, WI) in sterile Opti-modified Eagle's medium for 12 hours. Complete medium was then replaced for an additional 24 hours, and the cells were lysed using a solution of 4% Triton X-100, glycylglycine 100 mM, MgSO₄ 100 mM, and ethylene glycol tetraacetic acid 250 mM for 1 hour at room temperature on a shaker platform. The extracts were then combined with the solution containing the substrate (luciferin 2.5 mM and adenosine triphosphate 20 mM; Sigma-Aldrich) and analyzed with a luminometer (Lumat LB950; EG&G Berthold, Germany). AP-1-luciferase was bought from Takara Bio USA; pcDNA3.1-PPAR γ was a gift from Dr. V.K. Chatterjee (Department of Medicine, University of Cambridge, Addenbrooke's Hospital, Cambridge, United Kingdom); and pSG5-LXR α , pSG5-LXR β , and DR4-thymidine kinase luciferase were generous gifts from Dr. David Mangelsdorf (University of Texas Southwestern Medical Center, Dallas, TX). The pSG5 Vector is a eukaryotic expression vector constructed by combining pKCR2 and the Stratagene pBS vector. In this case either human LXR α or β were cloned into this vector.

STATISTICAL ANALYSIS

Unless otherwise indicated, data presented as bar graphs are the mean \pm SD of at least two independent experiments performed in triplicates. Three separated primary HSC isolations and three different clones carrying either WT or I148M *PNPLA3* genotypes were used (n = 3 for each genotype). Statistical analysis was performed using GraphPad Prism (La Jolla, CA). The unpaired Student *t* test was used when two groups were compared, and two-way analysis of

variance was used for multiple groups. *P* < 0.05 was considered statistically significant.

Results

PRIMARY HUMAN HSCs CARRYING THE *PNPLA3* I148M VARIANT DISPLAY REDUCED LXR α EXPRESSION AND TRANSCRIPTIONAL ACTIVITY COMPARED TO WT s

Because the nuclear receptor LXR exerts anti-inflammatory and antifibrotic actions in HSCs and the lack of LXR results in exacerbated liver fibrosis *in vivo*,⁽²¹⁾ we investigated the expression pattern of the two known isotypes LXR α and LXR β during human primary HSC activation *in vitro*. Interestingly, the LXR α protein amount increased progressively along with the profibrogenic marker α -smooth muscle actin (α -SMA) (Fig. 1A) during HSC activation, whereas LXR β was more abundant in the early phases (day 3 after isolation). In order to evaluate whether this finding corresponded to increased transcriptional LXR activity, we measured two key LXR target genes, adenosine triphosphate-binding cassette subfamily A, member 1 (ABCA1) and SREBP-1c. Interestingly, both LXR target genes were down-regulated, as reflected by significantly reduced ABCA1 (*P* < 0.001) expression in myofibroblast-like cells (HSCs 15 days after isolation) compared to quiescent HSCs (or freshly isolated HSCs; Fig. 1B), thus indicating reduced LXR functionality during HSC activation.

Given the influence of the *PNPLA3* genetic variant to the altered phenotype of HSC,⁽¹⁰⁾ we next compared the expression of LXR α and LXR β , evaluated by RT-PCR, western blotting, and immunofluorescence (IF) intracellular staining, among primary HSCs with the two different *PNPLA3* genotypes. Interestingly, we found significantly lower LXR α expression in *PNPLA3* I148M cells compared to WT HSCs (Fig. 1C-E).

In a pilot series, we also evaluated the amount of LXR α IF staining in NASH liver biopsies with different degrees of fibrosis and classified according to WT or I148M *PNPLA3* genotype. Total LXR α

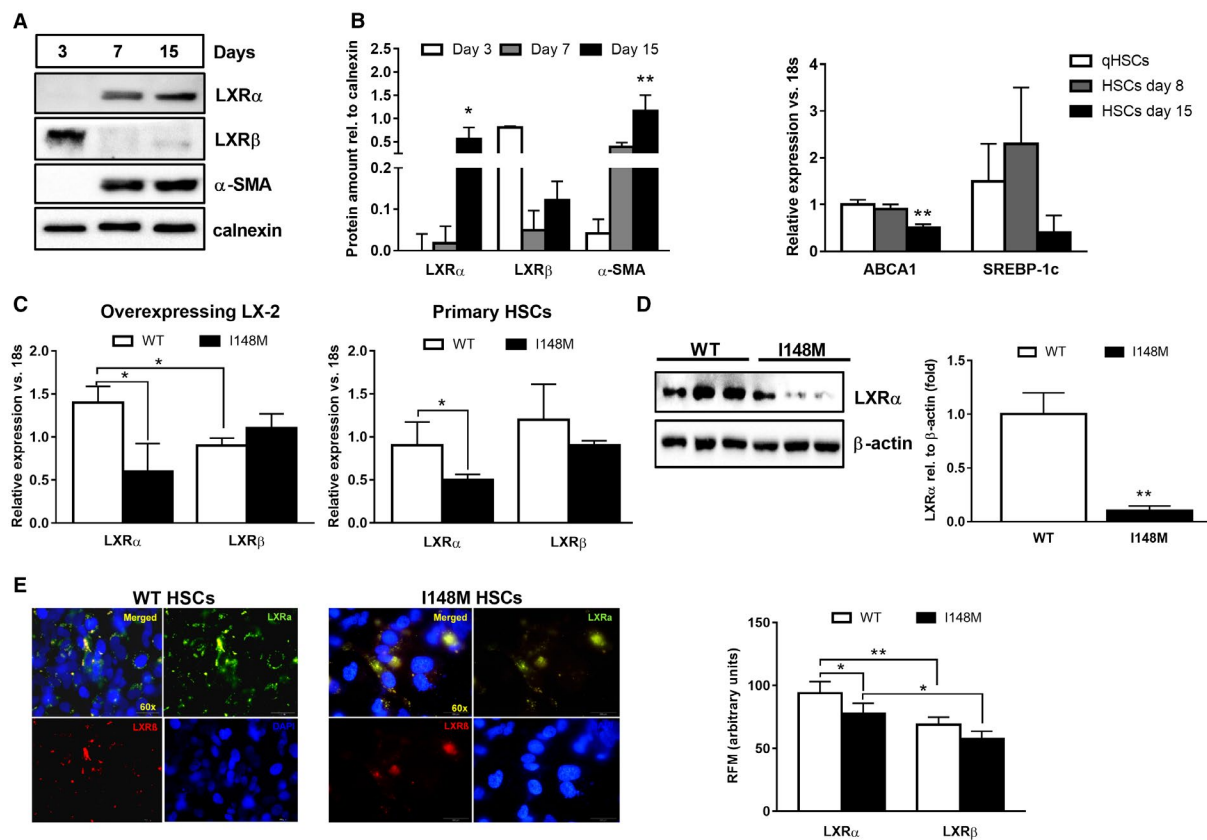


FIG. 1. Decreased LXR α transcriptional activity during human HSC activation and in *PNPLA3* I148M HSCs compared to WT. Human primary HSCs isolated from liver resections and cultivated *in vitro*, as described in Materials and Methods. All bar graphs show mean values \pm SD. (A) During *in vitro* activation (3, 7, and 15 days after cell isolation), cells were harvested and total protein extracts were used to detect LXR α , LXR β , α -SMA, and calnexin by western blotting. Blots are representative of three independent cell isolations. Densitometry analysis of blots was performed using ImageJ software, and results were normalized to calnexin. Data presented as protein amount relative to calnexin. Open bars show results for 3 days, gray bars for 7 days, and black bars for 15 days after isolation. * $P < 0.05$, ** $P < 0.01$ versus day 3. (B) ABCA1 and SREBP-1c mRNA expression analyzed by RT-PCR and data normalized to 18s. Freshly isolated cell data are depicted in white bars, 8 days after isolation data in gray bars, and 15 days after isolation in black bars ($n = 3$ independent isolations). ** $P < 0.01$ versus qHSCs. (C,D) Whole-cell extracts isolated from primary fully activated HSCs and stably overexpressing LX-2 ($n = 3$ for each *PNPLA3* genotype), as indicated in the figure. Expression of both LXR α and LXR β analyzed by RT-PCR and western blotting. Data normalized to 18s and β -actin for mRNA and protein, respectively. Open bars refer to *PNPLA3* WT HSCs and closed bars to I148M HSCs. Representative blots displayed. * $P < 0.05$, ** $P < 0.01$ versus WT HSCs. (E) Immunofluorescence staining shows intracellular localization of LXR α (Alexa 488, green) and LXR β (Alexa 568, red) in untreated human primary HSCs ($n = 3$ for each *PNPLA3* genotype). DAPI (blue) stains the nuclei. Merged (yellow) picture shows overlapping green and red channels. Magnification $\times 60$, and only representative images displayed. Quantitative RFM for LXR α (green channel) and LXR β (red channel) was calculated from representative pictures ($n = 6$ from each glass coverslip) using ImageJ software. Open bars refer to *PNPLA3* WT HSCs and closed bars to I148M HSCs. * $P < 0.05$ and ** $P < 0.01$, as indicated in the bar graph. Abbreviations: DAPI, 4',6-diamidino-2-phenylindole; qHSC, freshly isolated HSC; rel., relative; RFM, relative fluorescence mean.

expression was higher in patients carrying the variant compared to WT and correlated with a higher degree of steatosis but only partially colocalized with the HSC activation marker α -SMA (data not

shown). Collectively, our data established that LXR transcriptional activity is lowered during human HSC activation and diminishes in the presence of the *PNPLA3* I148M variant compared to WT HSCs.

DECREASED LXR SIGNALING DISRUPTS CHOLESTEROL HOMEOSTASIS IN HUMAN HSCs WITH *PNPLA3* I148M

To explore the functional impact of reduced LXR amount in *PNPLA3* I148M HSCs, we analyzed downstream targets of LXR, which could be separated into the following two main categories⁽²⁷⁾: (1) cholesterol efflux transporters ABCA1 and ABCG1^(30,31) and (2) *de novo* lipogenic genes (SREBP-1c, fatty acid synthase [FASN], and stearoyl-coenzyme A desaturase 1 [SCD1]). Gene expression analysis showed a significantly lower ABCA1 expression in I148M HSCs

(Fig. 2A), with no significant effect on ABCG1 and ABCG4 (Supporting Fig. S1). In addition, because oxysterols are natural ligands of LXR, we measured the gene expression of three pivotal enzymes producing LXR-activating oxysterols. Interestingly, primary HSCs carrying I148M *PNPLA3* showed a significant reduction of cytochrome P450 family 27, subfamily A, member 1 (CYP27A1; sterol 27-hydroxylase) and cholesterol 25-hydroxylase (CH25H) expression (Fig. 2B), suggesting a reduction in oxysterol generation.

Intracellular FC accumulation sensitizes HSCs to profibrogenic actions of TGF- β stimulation and promotes liver fibrosis development *in vivo*.⁽¹¹⁾ To determine whether the genetic variant of *PNPLA3* has

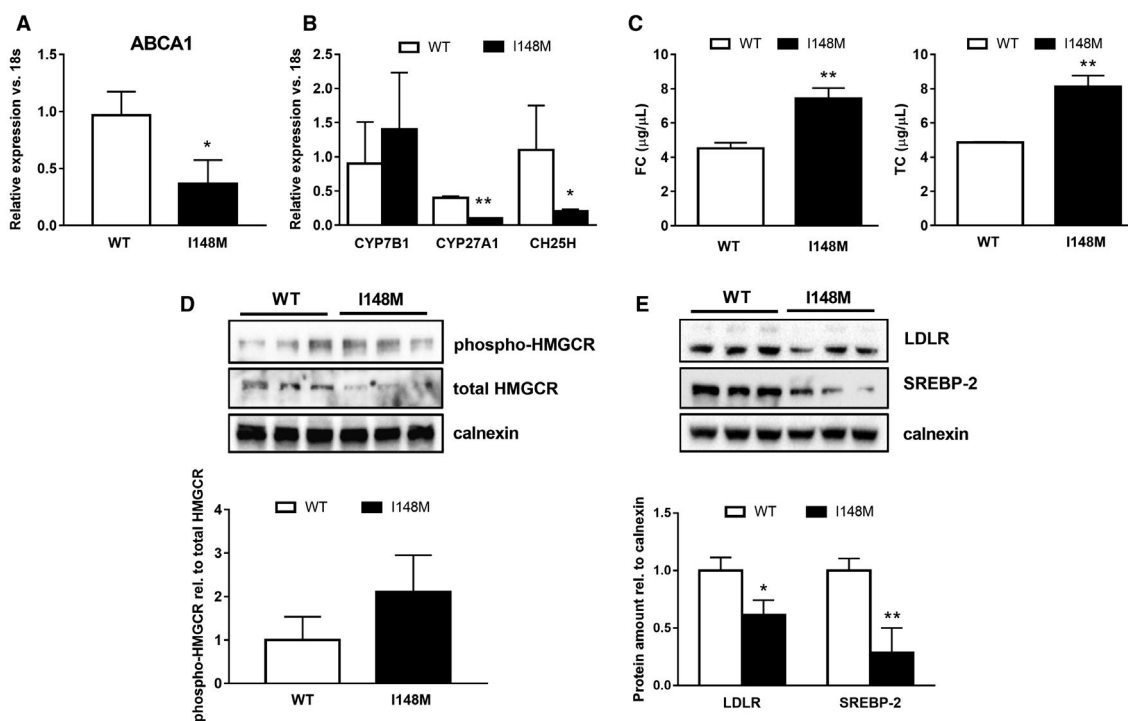


FIG. 2. Decreased LXR signaling disrupts cholesterol homeostasis in *PNPLA3* I148M carrying human HSCs. Human primary HSCs isolated from liver resections and cultivated *in vitro* and LX-2 stably overexpressing cells ($n = 3$ for each *PNPLA3* genotype) obtained, as described in Materials and Methods. All bar graphs show mean values \pm SD. (A,B) Expression of cholesterol efflux transporter ABCA1 and cholesterol-metabolizing enzymes CYP7B1, CYP27A1, and CH25H analyzed by RT-PCR and normalized to 18s in untreated primary HSCs carrying either the WT or the variant of *PNPLA3* ($n = 3$ for each genotype); * $P < 0.05$, ** $P < 0.01$. (C) TC and FC amounts quantified by using colorimetric quantitative assay on total lipid extracts collected from HSCs carrying either WT or I148M *PNPLA3*. Data shown are representative of two independent lipid extractions normalized to internal standards (Abcam); ** $P < 0.01$. (D,E) Total protein extracts were isolated from primary HSCs carrying either WT or I148M *PNPLA3* ($n = 3$ for each genotype) and analyzed by western blotting for SREBP-2, LDLR, phospho-HMGCR, and total HMGCR. Densitometry analysis was performed using ImageJ software, and data were normalized to calnexin. Data presented as protein amount relative to calnexin. Phospho-HMGCR was normalized to total HMGCR and expressed as protein ratio. Open bars refer to *PNPLA3* WT HSCs and closed bars to I148M HSCs ($n = 3$ for each genotype); * $P < 0.05$, ** $P < 0.01$ versus WT carriers. Abbreviations: phospho-, phosphorylated; rel., relative.

consequences on cholesterol metabolism and homeostasis in HSCs, we measured the TC and FC content in stably overexpressing WT and I148M LX-2. First, we found a significant increase of TC ($P < 0.01$) and FC ($P < 0.01$) content in cells carrying the *PNPLA3* variant (Fig. 2C). Endogenous cholesterol synthesis is regulated by HMGCR, which represents the rate-limiting step of the mevalonate pathway, and due to its central role, HMGCR is finely tuned and turned off by phosphorylation on a specific site (S872). Consistently, the ratio of phosphorylated HMGCR/total HMGCR is higher in HSCs carrying the variant (Fig. 2D), and this is supported by decreased messenger RNA (mRNA) as well (Supporting Fig. S2). Thereafter, we investigated the transcriptional activity of SREBP-2, a key sensor and modulator of intracellular cholesterol content. SREBP-2 gene expression (Supporting Fig. S1) and protein levels (Fig. 2E) were significantly lowered ($P < 0.05$, $P < 0.01$, respectively) in HSCs carrying the *PNPLA3* variant, in line with higher TC and FC content. Accordingly, SREBP-2 downstream target LDLR was significantly diminished at protein levels (Fig. 2E). Moreover, expression of *de novo* lipogenic genes and downstream targets of LXR, such as FASN, SCD1, and SREBP-1c, decreased in primary as well as in overexpressing *PNPLA3* variant HSCs (Supporting Fig. S2).

Notably, expression of acyl-coenzyme A:cholesterol acyltransferase 1 (ACAT1) and Niemann-Pick disease, type C intracellular cholesterol transporter 1 (NPC1) was profoundly down-regulated ($P < 0.01$) in primary HSCs carrying the *PNPLA3* variant, thus supporting that augmented FC content might result from decreased esterification to cholesterol esters (CEs) (Supporting Fig. S1). Therefore, based on the latter observations, we might conclude that LXR signaling is decreased due to diminished endogenous ligand generation, leading to accumulation of both TC and FC in HSCs expressing the genetic variant of *PNPLA3*.

LXR TRANSCRIPTIONAL ACTIVITY IS IMPAIRED IN *PNPLA3* I148M HSCs DUE TO LACK OF UPSTREAM PPAR γ FUNCTIONALITY

Ozasa et al.⁽²⁴⁾ and Chinetti and coworkers⁽³⁰⁾ reported the tight connection between PPAR γ and LXR axes in controlling ABCA1 expression in

human macrophages. Along with the findings published from our group on impaired PPAR γ signaling in the *PNPLA3* variant promoting higher proinflammatory cytokine release,⁽¹⁰⁾ we further explored whether PPAR γ 1 (the major isoform in HSCs) inhibition was contributing also to the reduced LXR transcriptional activity in cells carrying the *PNPLA3* genetic variant. Notably, in comparison to WT cells, LXRE-luciferase reporter activity was reduced and could not be significantly induced even in the presence of exogenous LXR in I148M HSCs (Fig. 3A). In addition, AP-1-luciferase activity increased significantly (2-fold) in cells expressing I148M *PNPLA3* and was inhibited after LXR agonist T09 treatment (Fig. 3B). Furthermore, analysis of the PPRE using the luciferase assay revealed that HSCs carrying the *PNPLA3* variant showed almost a 50% reduction for PPAR γ transcriptional activity, which could not be rescued by using either LXR or PPAR γ synthetic agonists T09 and ROSI, respectively (Fig. 3C). In contrast, endogenous LXR stimulation by T09 treatment induced LXRE-luciferase activity in *PNPLA3* WT and I148M cells and virtually normalized LXR signaling in both *PNPLA3* genotypes (Fig. 3D, panel LXRE vs. LXRE+T09; no significant difference between WT and I148M after T09), whereas ROSI increased LXRE-luciferase activity only in WT HSCs (Fig. 3D, LXRE+ROSI; significant difference between WT and I148M in LXRE-luciferase activity). Taken together, these data suggest that the lack of endogenous LXR ligand could explain impaired LXR signaling in I148M *PNPLA3* cells and that PPAR γ ligand increases LXR signaling only in WT cells.

SYNTHETIC LXR AGONIST T09 INDUCES LXR DOWNSTREAM TARGETS INDEPENDENTLY FROM PPAR γ IN BOTH WT AND I148M *PNPLA3* HSCs

In order to further explore and confirm our observations on the different responses induced by T09 and ROSI on LXRE, we stimulated cells with T09 and compared LXR target gene expression in WT and I148M *PNPLA3* HSCs. Stimulation with the synthetic LXR agonist T09 alone showed a significant induction of ABCA1 and reduction of profibrogenic markers collagen1 α 1 and chemokine (C-C motif)

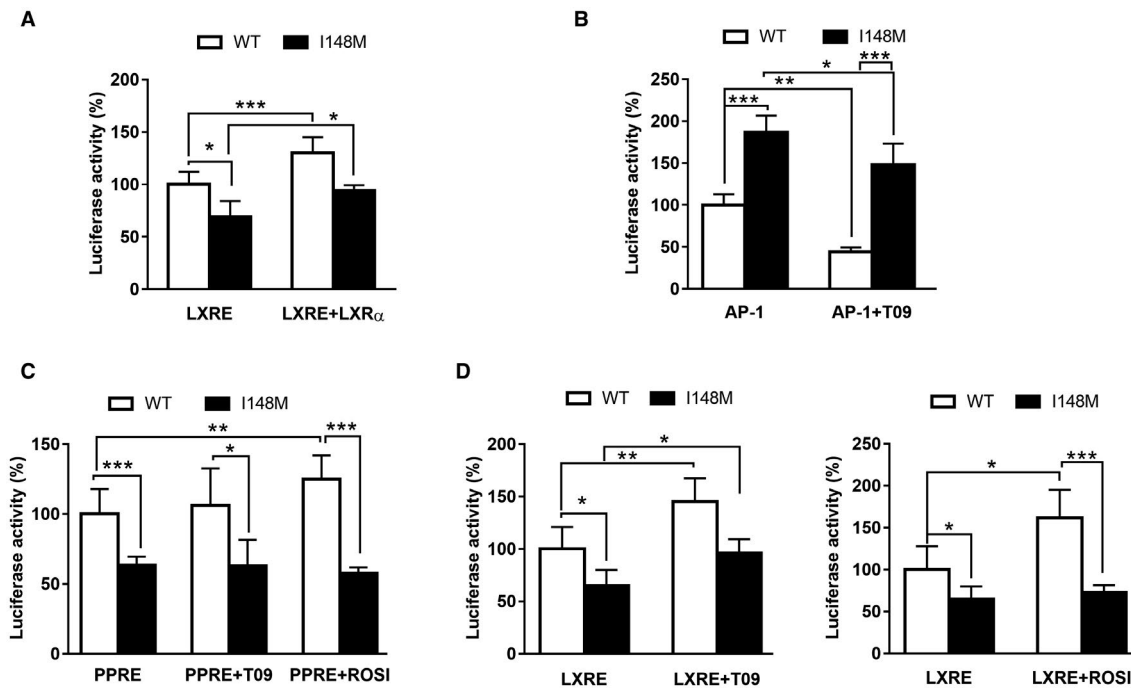


FIG. 3. LXR transcriptional activity is lower due to impaired PPAR γ 1 functionality in HSCs carrying *PNPLA3* I148M. LX-2 cells stably overexpressing WT or I148M *PNPLA3* transiently transfected with either LXRE, AP-1, or PPRE plasmids to measure LXR, AP-1, or PPAR γ transcriptional activity, respectively. After 48 hours, luciferase activity (expressed as percentage) was measured using a luminometer and normalized to total protein content, as described in Materials and Methods. All bar graphs show mean values \pm SD. (A) LXRE-luciferase activity was measured either in untreated HSCs or in the presence of nuclear receptor LXR (LXRE+LXR) for 24 hours. (B) AP-1-luciferase activity was measured either in untreated HSCs or in the presence of the synthetic LXR agonist T09 for 24 hours. (C) PPAR γ -luciferase activity was measured in untreated (PPRE) or previously treated HSCs with either T09 (PPRE+T09) or rosiglitazone (PPRE+ROSI) for 24 hours. (D) LXRE-luciferase activity was measured in untreated (LXRE) or in pretreated HSCs with either 10 nM of T09 (LXRE+T09) or rosiglitazone (LXRE+ROSI) for 24 hours. All bar graphs are representative of four independent transfections performed in triplicates. * $P < 0.05$, ** $P < 0.01$, and *** $P < 0.001$, as indicated in the bar graphs. Open bars refer to *PNPLA3* WT HSCs and closed bars to I148M HSCs ($n = 3$ for each genotype).

ligand 5 (CCL5) in WT-expressing HSCs ($P < 0.001$; Fig. 4, left panels, gray bars). Similarly, T09 also significantly promoted ABCA1 expression and decreased collagen1 α 1 and CCL5 in I148M variant HSCs ($P < 0.001$; Fig. 4, right panels, gray bars). Interestingly, the addition of ROSI to T09 showed further induction of ABCA1 expression only in WT cells ($P < 0.001$; Fig. 4, left panels, black bars) and displayed consistent reduction of collagen1 α 1 and CCL5 as the stimulation with T09 alone, supporting the hypothesis that PPAR γ positively affects LXR target gene expression. In contrast to WT *PNPLA3* HSCs, *PNPLA3* I148M variant cells stimulated with T09 in combination with ROSI did not display higher ABCA1 and diminished collagen1 α 1 and CCL5 ($P < 0.05$ and $P < 0.001$, respectively; Fig. 4, right panels, black bars). These observations, therefore, suggest that T09 induces

LXR signaling in HSCs carrying I148M *PNPLA3* whereas ROSI has these beneficial effects only in WT *PNPLA3* HSCs.

SPECIFIC LXR INVERSE AGONIST SR9238 AND ANTAGONIST GSK2033 BLOCK LXR SIGNALING IN WT AND I148M *PNPLA3* HSCs

Because T09 is also known to have LXR off-targeting effects involving farnesoid X receptor (FXR) and pregnane X receptor (PXR)^(32,33) and to evaluate the specificity of LXR signaling and the positive effects shown by the LXR agonist T09 in human HSCs, we used a specific synthetic LXR inverse agonist (SR9238) and LXR antagonist (GSK2033) to block LXR signaling in both WT and I148M HSCs.

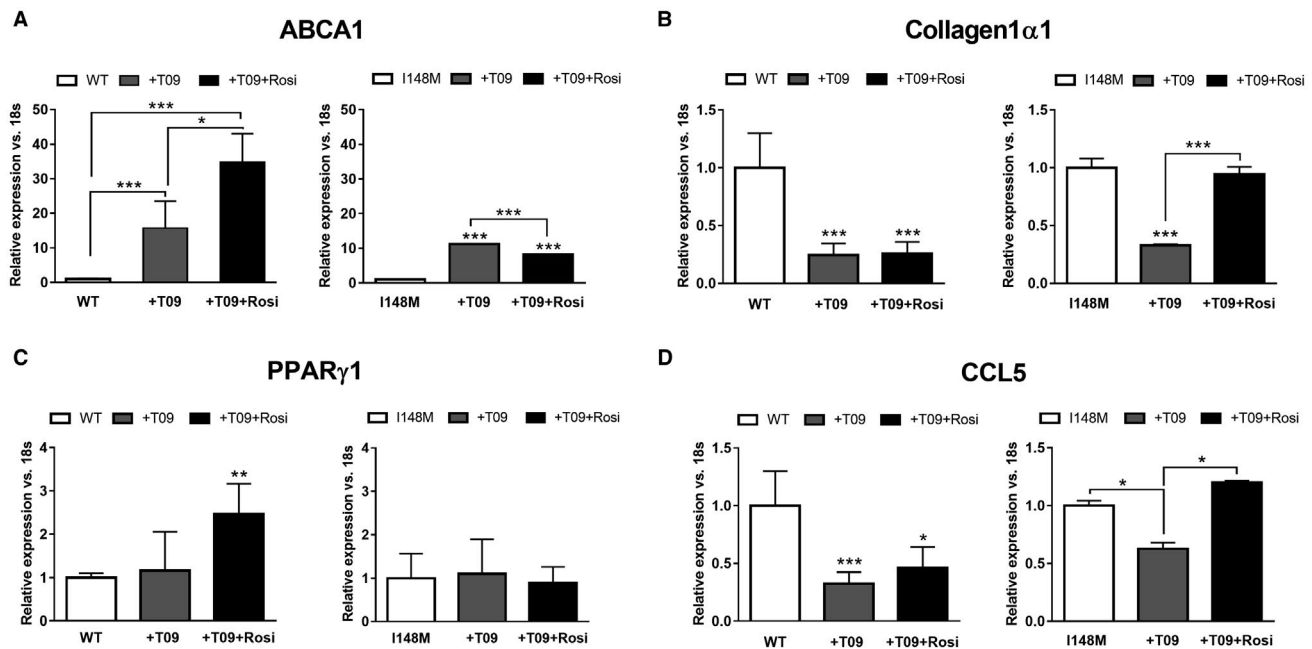


FIG. 4. LXR agonist T09 alone restores ABCA1 and attenuates inflammatory and fibrogenic markers independently from PPAR γ in HSCs with the *PNPLA3* I148M variant. LX-2 stable overexpressing WT or I148M *PNPLA3* untreated or treated for 24 hours with either T09 (+T09) or the combination T09 and ROSI (+T09+Rosi). mRNA expression of (A) ABCA1, (B) collagen1 α 1, (C) PPAR γ 1 and (D) CCL5 and analyzed by RT-PCR and normalized to 18s. White bars show untreated HSCs, gray bars show HSCs treated with T09, and black bars show HSCs treated with T09 or the combination (+T09+Rosi). All bar graphs show mean values \pm SD. * P < 0.05, ** P < 0.01, and *** P < 0.001 versus untreated WT or I148M HSCs (n = 3 for each genotype).

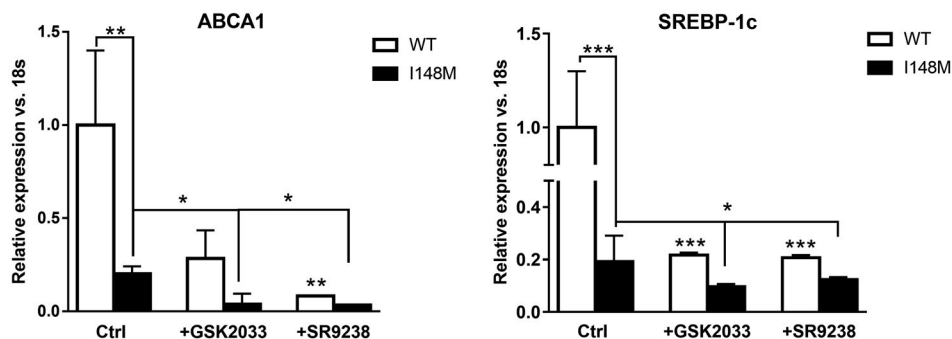


FIG. 5. LXR inverse agonist SR9238 and antagonist GSK2033 blocked T09-induced LXR signaling in human HSCs. Whole mRNA extract collected from untreated (ctrl) stably overexpressing LX-2 carrying either WT or I148M *PNPLA3*, treated with LXR inverse agonist (SR9238) or LXR antagonist (GSK2033) for 24 hours. Expression of ABCA1 and SREBP-1c analyzed by RT-PCR and normalized to 18s. I148M expression data were normalized to WT ctrl. All bar graphs show mean values \pm SD. * P < 0.05, ** P < 0.01, and *** P < 0.001 versus untreated WT HSCs or as indicated in the graph. Abbreviation: Ctrl, control.

In WT HSCs, both SR9238 and GSK2033 significantly reduced ABCA1 and SREBP-1c expression (P < 0.05, P < 0.01, respectively; Fig. 5, white bars). In contrast to the positive actions of T09, both GSK2033 and SR9238 resulted in a significant decrease in

ABCA1 and SREBP-1c expression also in I148M *PNPLA3* HSCs (P < 0.05, P < 0.01, respectively; Fig. 5, black bars). Taken together, these data established the role of LXR signaling in the regulation mediated by the T09 agonist.

ROSI PROMOTES LXR SIGNALING AND DECREASES INFLAMMATORY CYTOKINE EXPRESSION ONLY IN HSCs EXPRESSING WT *PNPLA3*

Data collected by our group have highlighted the impact of the genetic variant of *PNPLA3* in inducing a proinflammatory phenotype in human HSCs.⁽¹⁰⁾ Because activation of LXRs attenuates inflammation and inflammatory gene expression in many cell types⁽³⁴⁾ and ROSI positively regulates LXRE in WT but not in I148M-expressing cells (Figs. 3D and 4), we speculated that activation of PPAR γ controls LXRs and the downstream targets in WT *PNPLA3* cells but not in I148M cells. To test the hypothesis, we next treated HSCs with ROSI only (Fig. 6). Interestingly, PPAR γ synthetic agonist up-regulated ABCA1 expression in both WT and I148M HSCs but LXR α only in WT cells (Fig. 6A), thus suggesting that the partial recovery of LXRE shown in Fig. 3D resulted in induction of specific gene sets.

Consistently, ROSI positively influenced the expression of the LXR α downstream lipogenic gene FASN only in WT *PNPLA3*-expressing HSCs, whereas SREBP-1c in I148M cells was not increased (Fig. 6A), thus supporting that PPAR γ /LXR signaling crosstalk was blunted in I148M cells, which might be partially recovered by ROSI. Importantly, the treatment significantly decreased ($P < 0.001$) expression of proinflammatory cytokines, such as CCL2, CCL5, and interleukin-8 (IL-8), only in WT but not I148M HSCs (Fig. 6B), consistent with our observations on the posttranslational modification of PPAR γ by phosphorylation in HSCs carrying I148M⁽¹⁰⁾ and the luciferase data (Fig. 3D). Collectively, our observations suggest that I148M *PNPLA3* lacks LXR activation, probably due to weak oxysterol synthesis, resulting in accumulation of FC and TC. In addition, stimulation with synthetic agonists showed distinct effects on PPAR γ and LXR target gene expressions, suggesting that lack of PPAR γ activation upstream represses LXR activity whereas direct activation of LXR with its specific agonist T09 results in significantly higher

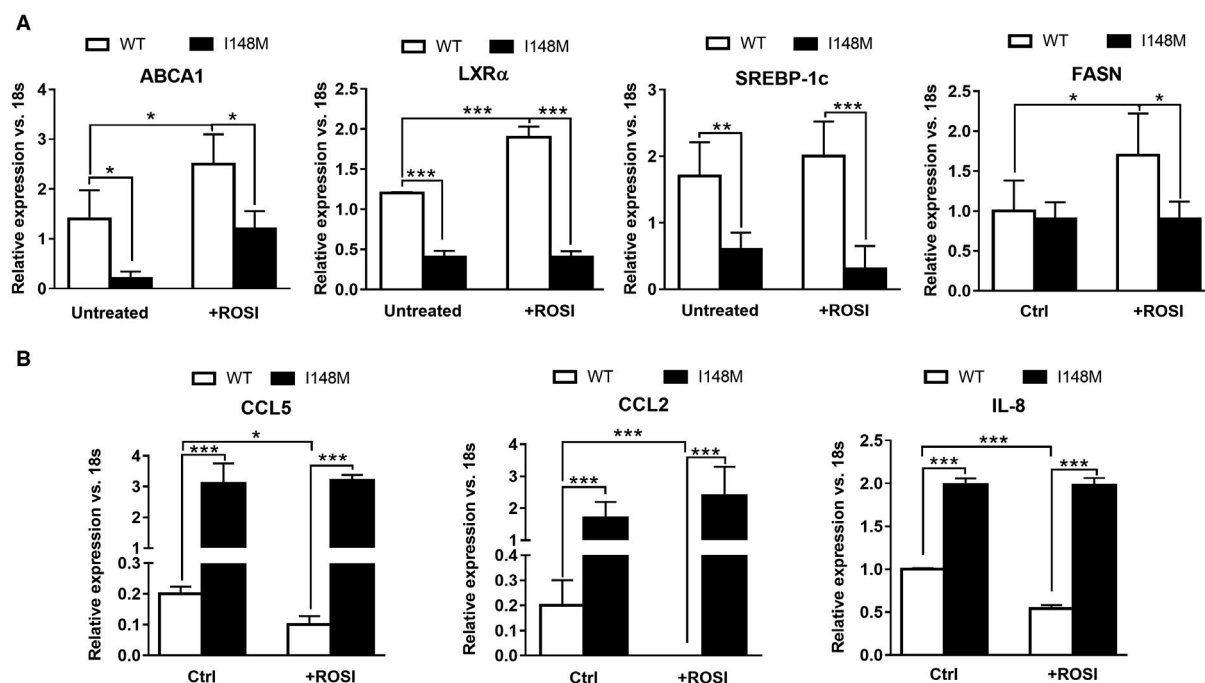


FIG. 6. ROSI up-regulates LXR α prolipogenic genes and reduces inflammatory cytokine expressions only in WT but not I148M HSCs. Whole mRNA extract collected from untreated stably overexpressing LX-2 carrying either WT or I148M *PNPLA3* or treated with ROSI for 24 hours. All bar graphs show mean values \pm SD. (A) Expression of ABCA1, LXR α , SREBP-1c, and FASN analyzed by RT-PCR and normalized to 18s. (B) Expression of CCL5, CCL2, and IL-8 analyzed by RT-PCR and normalized to 18s. Data displayed represent two independent experiments performed in triplicates. White bars refer to *PNPLA3* WT HSCs and black bars to I148M ($n = 3$ for each genotype); * $P < 0.05$, ** $P < 0.01$, and *** $P < 0.001$. Abbreviation: Ctrl, control.

ABCA1 and less collagen1 α 1 and CCL5 expression in HSCs carrying the I148M variant (Fig. 7).

Discussion

Our findings report novel mechanistic aspects explaining the impact of the genetic variant I148M on LXR nuclear receptor signaling and cholesterol metabolism in human HSCs. The genetic variant of *PNPLA3* results in phosphorylation of PPAR γ on specific inhibitory residue, down-regulating its transcriptional activity, and impairing the downstream functionality of the two isotypes of LXRs. In addition, decreased LXR signaling diminishes intracellular cholesterol efflux (through ABCA1) and *de novo* lipogenesis (through SREBP-1c) and promotes accumulation of toxic FC and TC, which are not metabolized to oxysterols (by CYP27A1, CYP7B1 [known also as 25-hydroxycholesterol 7- α -hydroxylase], and CH25H) or esterified to CEs (by ACAT1). Altogether, HSCs carrying I148M *PNPLA3* show enhanced expression of proinflammatory mediators (CCL2, CCL5, and IL-8), proliferation, and migration capability.⁽¹⁰⁾

Oxysterols represent the natural ligands for LXR nuclear receptors⁽²⁵⁾ and have been shown to control lipid metabolism and cholesterol homeostasis in different cell types and tissues.⁽²⁰⁾ In particular, LXRs regulate

lipogenic and inflammatory pathways in HSCs because lack of LXR signaling resulted in impaired lipid partitioning and increased fibrogenic and inflammatory cytokine expression *in vitro* and *in vivo*.⁽²¹⁾ Analyzing LXRs during early *in vitro* activation of freshly isolated human HSCs revealed that LXR α increased along with α -SMA whereas the β isotype decreased (Fig. 1A). Nevertheless, LXR downstream targets are down-regulated during HSC *in vitro* activation, thus suggesting that the transcriptional activity of this nuclear receptor diminishes when HSCs achieve a fully activated myofibroblast phenotype (Fig. 1B-E), in line with the data published by Beaven et al.⁽²¹⁾ It is important to consider that both LXR isotypes show a different distribution in the human body, thus suggesting a potential distinct tissue-specific or even cell-specific role according to their localization. Moreover, they regulate an overlapping set of genes and therefore might act synergistically or compensate for each other.⁽¹⁹⁾ Mice lacking LXR α display accumulation of CEs when challenged with a high-cholesterol diet. This proves that LXR α controls hepatic lipid metabolism through SREBP-1c^(18,35) and promotes reverse cholesterol transport and excretion.⁽²⁶⁾ In this regard, specific analysis of primary and overexpressing HSCs revealed that LXR α (mRNA, protein content, and intracellular amount; Fig. 1C-E) is significantly lower in HSCs with the *PNPLA3* genetic variant, in line with the histologic evaluation in human liver biopsies (data not shown). Our first

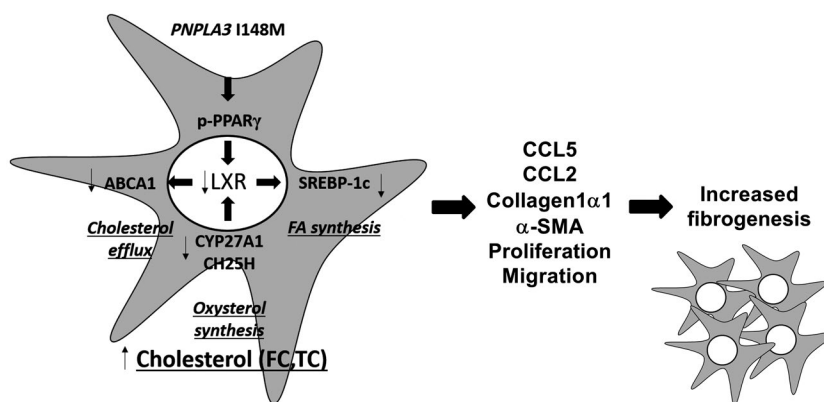


FIG. 7. Summary representation of impaired LXR α signaling resulting in altered TC and FC accumulation in human HSCs carrying I148M *PNPLA3*. Activated human HSCs carrying I148M have decreased PPAR γ transcriptional activity due to phosphorylation on specific inhibitory residue (p-PPAR γ), which directly impairs LXR target gene expression involved in cholesterol and lipid metabolism (ABCA1, SREBP-1c, FASN). As such, reduced cholesterol efflux through ABCA1 leads to TC and FC accumulation, accompanied by reduced endogenous cholesterol synthesis (SREBP-2, HMGCR) and decreased extracellular uptake (LDLR). Reduced PPAR/LXR signaling axis decreases the anti-inflammatory ability of these nuclear receptors, thus resulting in higher expression of profibrogenic features (CCL5, CCL2, collagen1 α 1, α -SMA, increased migration and proliferation).

findings during HSC *in vitro* activation led us to investigate the LXR downstream targets in WT and I148M HSCs. ABCA1 (Fig. 2A), SREBP-1c, FASN, and SCD1 (Supporting Figs. S1 and S2) were diminished in HSCs carrying the *PNPLA3* genetic variant. In comparison with WT HSCs, the evidence of lower LXR activity was supported by reduced expression levels of oxysterol-releasing enzymes CYP27A1⁽³⁶⁾ and CH25H^(36,37) (Fig. 2B), which is consistent with the hypothesis that a lack of endogenous LXR ligands contributes to their decreased expression and transcriptional activity.

Dysregulation of hepatic triglyceride metabolism and impaired cholesterol homeostasis are widely recognized as active players in the development of NAFLD. Notably, increased intracellular FC accumulation positively correlates with the transition from simple steatosis toward NASH⁽³⁸⁻⁴¹⁾ and with exacerbated HSC-mediated liver fibrogenesis in mice fed a high-cholesterol diet in two different models of hepatic fibrosis.^(11,12) At baseline, HSCs isolated from these mice already show increased FC accumulation, which sensitizes HSCs to TLR4 signaling, leading to down-regulation of BAMBI and a faster response to profibrogenic actions of TGF- β .⁽¹¹⁾ FC derives from three main sources: increased endogenous synthesis, improved extracellular uptake, and decreased efflux. Intracellular cholesterol levels finely regulate the transcriptional activity of SREBP-2. In the nucleus, SREBP-2 positively induces the expression of the enzymes for cholesterol synthesis and uptake, HMGCR, 3-hydroxy-3-methylglutaryl coenzyme A synthase (HMGCS), and LDLR.⁽³⁹⁾ In line with the TC and FC accumulation, our gene and protein analysis revealed that the I148M *PNPLA3*-carrying HSCs displayed lower SREBP-2 transcriptional activity in both primary and overexpressing cells, as suggested by decreased LDLR, HMGCR, and HMGCS expressions (Fig. 2D,E; Supporting Figs. S1 and S2). Remarkably, according to other observations,⁽¹³⁾ diminished ACAT1 and NPC1 expressions in HSCs carrying I148M contribute to accumulated FC in HSCs (Supporting Fig. S1), thus playing a role in liver fibrogenesis. In addition, KO HSCs for NPC1 accumulate FC and are more sensitive to TGF- β -induced collagen1 α 1 and α -SMA expressions.⁽¹³⁾

Interestingly, our transfections data pointed out that LXRE transcriptional activity was impaired in I148M-carrying HSCs, even when an LXR α plasmid

was added (Fig. 3), reflecting the lower content of ligands activating this transcription factor in these cells. In particular, the contribution of diminished PPAR γ signaling reported by our group⁽¹⁰⁾ and the transcriptional control of LXR by PPAR γ in macrophages⁽²⁹⁾ encouraged us to investigate whether a similar mechanism occurred in our HSCs with the *PNPLA3* variant. Indeed, only LXR activated by T09 achieved an up-regulation comparable to that found in WT HSCs on LXRE-luciferase without affecting the PPRE transactivation (Fig. 3C). Remarkably, WT HSCs display increased transcriptional activity of LXRE following both T09 and ROSI treatment whereas HSCs carrying the variant only following T09 treatment, underlying a possible role of PPAR γ upstream of LXR (Fig. 3D). Along with the latter data, T09 treatment significantly decreased AP-1 transcriptional activity in WT cells and had positive effects also in I148M HSCs, indicating a positive action mediated by partially reestablished LXR signaling, without affecting PPAR γ downstream targets (Fig. 3). Accordingly, stimulation with LXR synthetic agonist displayed positive effects on gene expression for ABCA1 and significantly reduced collagen1 α 1 and CCL5 in the HSCs of both *PNPLA3* genotypes (Fig. 4, gray bars), suggesting for the first time that restoring LXR signaling in *PNPLA3* I148M variant cells could be a potential strategy to repress fibrogenic features in these HSCs (Fig. 4, right panels, black bars).

Because T09 has LXR-independent effects mediated by FXR and PXR,^(32,33) the use of LXR-specific inverse agonist and antagonist was necessary to demonstrate that LXR was the key transcription factor involved in our findings. Indeed, LXR inverse agonist lowered ABCA1 and SREBP-1c expression below the control levels (Fig. 5) in WT HSCs. However, in I148M HSCs, the inverse agonist and the antagonist still had effects in decreasing expression of LXR targets but they were moderate compared to WT *PNPLA3* HSCs (Fig. 5), which could possibly be caused by reduced endogenous oxysterols activating LXR.

Considering the capacity of LXRs to repress release of inflammatory mediators in macrophages, the role of these nuclear receptors strongly leads to a link between hepatic metabolism and immune response. Liver resident macrophages lacking LXRs underline that the latter control the differentiation of the Kupffer cell population and regulate immune and

inflammatory responses in mice.^(22,41) The activation and overexpression of LXR α following ROSI stimulation provides a direct anti-inflammatory effect on cytokine expression in HSCs carrying the WT along with no detectable improvement in cells with the *PNPLA3* variant (Fig. 5B).

Collectively, our findings uncover I148M *PNPLA3* as an additional interesting contributor of impaired cholesterol and lipid metabolism in human HSCs, predisposing to exacerbated proinflammatory phenotype and enhanced hepatic fibrosis severity in humans. Of note, LXR α and LXR β regulate distinct and overlapping sets of genes and show high homology in their ligand-binding domains, thus reducing the possibilities to obtain subtype-specific agonists. New molecules were synthesized and revealed the impact of single isotype activation in therapeutic scenarios.⁽²⁷⁾ Novel approaches also include the use of inverse agonists for LXRs. In this regard, the SR9238 compound is effective in reducing hepatic steatosis, inflammation, and fibrosis in a model of murine steatohepatitis,⁽⁴²⁾ highlighting the potential implications in human NASH. To counteract intracellular cholesterol accumulation, another strategy might be the use of statins. Clinical studies on patients with NAFLD have demonstrated that statins have a positive impact by diminishing steatosis, NASH, and fibrosis, although the presence of the *PNPLA3* genetic variant blunted these beneficial effects.⁽⁴³⁾

Nevertheless, further molecular and *in vivo* studies are needed to address the specific contribution of the two LXR isotypes in HSCs expressing the *PNPLA3* variant, considering their pivotal role in controlling hepatic lipid machinery and innate immune response, and therefore leading to an alternative therapeutic approach beyond PPAR γ agonists.

Acknowledgment: We thank Peter Ferenci (Division of Gastroenterology and Hepatology, Department of Internal Medicine III, Medical University of Vienna, Vienna, Austria) for *PNPLA3* genotyping.

REFERENCES

- Cohen JC, Horton JD, Hobbs HH. Human fatty liver disease: old questions and new insights. *Science* 2011;332:1519-1523.
- Mann JP, Anstee QM. NAFLD: PNPLA3 and obesity: a synergistic relationship in NAFLD. *Nat Rev Gastroenterol Hepatol* 2017;14:506-507.
- Anstee QM, Seth D, Day CP. Genetic factors that affect risk of alcoholic and nonalcoholic fatty liver disease. *Gastroenterology* 2016;150:1728-1744.e1727.
- Bruschi FV, Tardelli M, Claudel T, Trauner M. PNPLA3 expression and its impact on the liver: current perspectives. *Hepat Med* 2017;9:55-66.
- Trepo E, Romeo S, Zucman-Rossi J, Nahon P. PNPLA3 gene in liver diseases. *J Hepatol* 2016;65:399-412.
- Schuster S, Cabrera D, Arrese M, Feldstein AE. Triggering and resolution of inflammation in NASH. *Nat Rev Gastroenterol Hepatol* 2018;15:349-364.
- Caligiuri A, Gentilini A, Marra F. Molecular pathogenesis of NASH. *Int J Mol Sci* 2016;17. pii:E1575.
- Yin C, Evason KJ, Asahina K, Stainier DY. Hepatic stellate cells in liver development, regeneration, and cancer. *J Clin Invest* 2013;123:1902-1910.
- Friedman SL. Hepatic stellate cells: protean, multifunctional, and enigmatic cells of the liver. *Physiol Rev* 2008;88:125-172.
- Bruschi FV, Claudel T, Tardelli M, Caligiuri A, Stulnig TM, Marra F, et al. The PNPLA3 I148M variant modulates the fibrogenic phenotype of human hepatic stellate cells. *Hepatology* 2017;65:1875-1890.
- Teratani T, Tomita K, Suzuki T, Oshikawa T, Yokoyama H, Shimamura K, et al. A high-cholesterol diet exacerbates liver fibrosis in mice via accumulation of free cholesterol in hepatic stellate cells. *Gastroenterology* 2012;142:152-164.e110.
- Tomita K, Teratani T, Suzuki T, Shimizu M, Sato H, Narimatsu K, et al. Free cholesterol accumulation in hepatic stellate cells: mechanism of liver fibrosis aggravation in nonalcoholic steatohepatitis in mice. *Hepatology* 2014;59:154-169.
- Tomita K, Teratani T, Suzuki T, Shimizu M, Sato H, Narimatsu K, et al. Acyl-CoA:cholesterol acyltransferase 1 mediates liver fibrosis by regulating free cholesterol accumulation in hepatic stellate cells. *J Hepatol* 2014;61:98-106.
- Apfel R, Benbrook D, Lernhardt E, Ortiz MA, Salbert G, Pfahl M. A novel orphan receptor specific for a subset of thyroid hormone-responsive elements and its interaction with the retinoid/thyroid hormone receptor subfamily. *Mol Cell Biol* 1994;14:7025-7035.
- Song C, Kokontis JM, Hiipakka RA, Liao S. Ubiquitous receptor: a receptor that modulates gene activation by retinoic acid and thyroid hormone receptors. *Proc Natl Acad Sci U S A* 1994;91:10809-10813.
- Wang B, Tontonoz P. Liver X receptors in lipid signalling and membrane homeostasis. *Nat Rev Endocrinol* 2018;14:452-463.
- Willy PJ, Umesono K, Ong ES, Evans RM, Heyman RA, Mangelsdorf DJ. LXR, a nuclear receptor that defines a distinct retinoid response pathway. *Genes Dev* 1995;9:1033-1045.
- Repa JJ, Mangelsdorf DJ. The role of orphan nuclear receptors in the regulation of cholesterol homeostasis. *Annu Rev Cell Dev Biol* 2000;16:459-481.
- Chawla A, Repa JJ, Evans RM, Mangelsdorf DJ. Nuclear receptors and lipid physiology: opening the X-files. *Science* 2001;294:1866-1870.
- Zelcer N, Tontonoz P. Liver X receptors as integrators of metabolic and inflammatory signaling. *J Clin Invest* 2006;116:607-614.
- Beaven SW, Wroblewski K, Wang J, Hong C, Bensinger S, Tsukamoto H, et al. Liver X receptor signaling is a determinant of stellate cell activation and susceptibility to fibrotic liver disease. *Gastroenterology* 2011;140:1052-1062.
- Endo-Umeda K, Nakashima H, Komine-Aizawa S, Umeda N, Seki S, Makishima M. Liver X receptors regulate hepatic F4/80 (+) CD11b(+) Kupffer cells/macrophages and innate immune responses in mice. *Sci Rep* 2018;8:9281.
- Janowski BA, Willy PJ, Devi TR, Falck JR, Mangelsdorf DJ. An oxysterol signalling pathway mediated by the nuclear receptor LXR alpha. *Nature* 1996;383:728-731.

- 24) Ozasa H, Ayaori M, Iizuka M, Terao Y, Uto-Kondo H, Yakushiji E, et al. Pioglitazone enhances cholesterol efflux from macrophages by increasing ABCA1/ABCG1 expressions via PPARgamma/LXRalpha pathway: findings from in vitro and ex vivo studies. *Atherosclerosis* 2011;219:141-150.
- 25) Lehmann JM, Kliewer SA, Moore LB, Smith-Oliver TA, Oliver BB, Su JL, et al. Activation of the nuclear receptor LXR by oxysterols defines a new hormone response pathway. *J Biol Chem* 1997;272:3137-3140.
- 26) Peet DJ, Turley SD, Ma W, Janowski BA, Lobaccaro JM, Hammer RE, et al. Cholesterol and bile acid metabolism are impaired in mice lacking the nuclear oxysterol receptor LXR alpha. *Cell* 1998;93:693-704.
- 27) Lund EG, Peterson LB, Adams AD, Lam MH, Burton CA, Chin J, et al. Different roles of liver X receptor alpha and beta in lipid metabolism: effects of an alpha-selective and a dual agonist in mice deficient in each subtype. *Biochem Pharmacol* 2006;71:453-463.
- 28) Huang Y, He S, Li JZ, Seo YK, Osborne TF, Cohen JC, et al. A feed-forward loop amplifies nutritional regulation of PNPLA3. *Proc Natl Acad Sci U S A* 2010;107:7892-7897.
- 29) **Chawla A, Boisvert WA, Lee CH, Laffitte BA**, Barak Y, Joseph SB, et al. A PPAR gamma-LXR-ABCA1 pathway in macrophages is involved in cholesterol efflux and atherosclerosis. *Mol Cell* 2001;7:161-171.
- 30) Chinetti G, Lestavel S, Bocher V, Remaley AT, Neve B, Torra IP, et al. PPAR-alpha and PPAR-gamma activators induce cholesterol removal from human macrophage foam cells through stimulation of the ABCA1 pathway. *Nat Med* 2001;7:53-58.
- 31) Klucken J, Buchler C, Orso E, Kaminski WE, Porsch-Ozcurumez M, Liebisch G, et al. ABCG1 (ABC8), the human homolog of the *Drosophila* white gene, is a regulator of macrophage cholesterol and phospholipid transport. *Proc Natl Acad Sci U S A* 2000;97:817-822.
- 32) Houck KA, Borchert KM, Hepler CD, Thomas JS, Bramlett KS, Michael LF, et al. T0901317 is a dual LXR/FXR agonist. *Mol Genet Metab* 2004;83:184-187.
- 33) Mitro N, Vargas L, Romeo R, Koder A, Saez E. T0901317 is a potent PXR ligand: implications for the biology ascribed to LXR. *FEBS Lett* 2007;581:1721-1726.
- 34) Michael DR, Ashlin TG, Buckley ML, Ramji DP. Liver X receptors, atherosclerosis and inflammation. *Curr Atheroscler Rep* 2012;14:284-293.
- 35) **Schultz JR, Tu H**, Luk A, Repa JJ, Medina JC, Li L, et al. Role of LXRs in control of lipogenesis. *Genes Dev* 2000;14:2831-2838.
- 36) Shanahan CM, Carpenter KL, Cary NR. A potential role for sterol 27-hydroxylase in atherogenesis. *Atherosclerosis* 2001;154:269-276.
- 37) Lund EG, Kerr TA, Sakai J, Li WP, Russell DW. cDNA cloning of mouse and human cholesterol 25-hydroxylases, polytopic membrane proteins that synthesize a potent oxysterol regulator of lipid metabolism. *J Biol Chem* 1998;273:34316-34327.
- 38) Arguello G, Balboa E, Arrese M, Zanlungo S. Recent insights on the role of cholesterol in non-alcoholic fatty liver disease. *Biochim Biophys Acta* 2015;1852:1765-1778.
- 39) **Musso G, Gambino R**, Cassader M. Cholesterol metabolism and the pathogenesis of non-alcoholic steatohepatitis. *Prog Lipid Res* 2013;52:175-191.
- 40) **Moon YA, Liang G**, Xie X, Frank-Kamenetsky M, Fitzgerald K, Kotliansky V, et al. The Scap/SREBP pathway is essential for developing diabetic fatty liver and carbohydrate-induced hypertriglyceridemia in animals. *Cell Metab* 2012;15:240-246.
- 41) Endo-Umeda K, Nakashima H, Umeda N, Seki S, Makishima M. Dysregulation of Kupffer cells/macrophages and natural killer T cells in steatohepatitis in LXRalpha knockout male mice. *Endocrinology* 2018;159:1419-1432.
- 42) Griffett K, Welch RD, Flaveny CA, Kolar GR, Neuschwander-Tetri BA, Burris TP. The LXR inverse agonist SR9238 suppresses fibrosis in a model of non-alcoholic steatohepatitis. *Mol Metab* 2015;4:353-357.
- 43) Dongiovanni P, Petta S, Mannisto V, Mancina RM, Pipitone R, Karja V, et al. Statin use and non-alcoholic steatohepatitis in at risk individuals. *J Hepatol* 2015;63:705-712.

Author names in bold designate shared co-first authorship.

Supporting Information

Additional Supporting Information may be found at onlinelibrary.wiley.com/doi/10.1002/hep4.1395/suppinfo.